FAST-FSSP

An improved version of the PMS FSSP-100

Brenguier, 1993,
J.A.M. 32, 783-793

Pawlowska et al., 1997,
J.A.O.T., 14, 88-104

Brenguier et al. 1998,
J.A.O.T., 15, 1077-1090

Brenguier & Chaumat, 2001,
J.A.S., **58**, 628-641.

Chaumat & Brenguier, 2001,
J.A.S., **58**, 642-654.

Burnet & Brenguier, 2002,
J.A.O.T., **in press**.

FSSP-100 Schematics

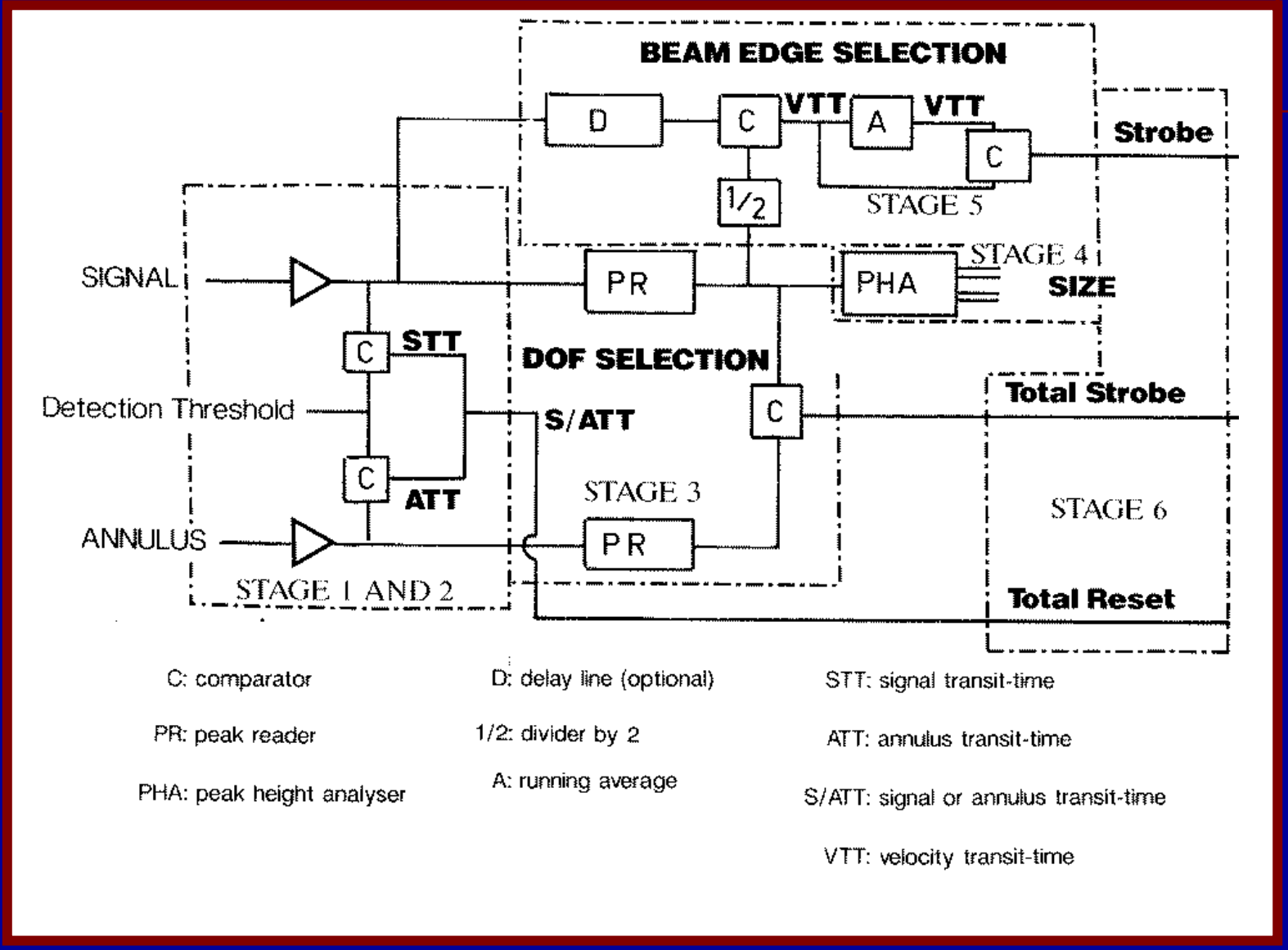

FAST-FSSP Schematics

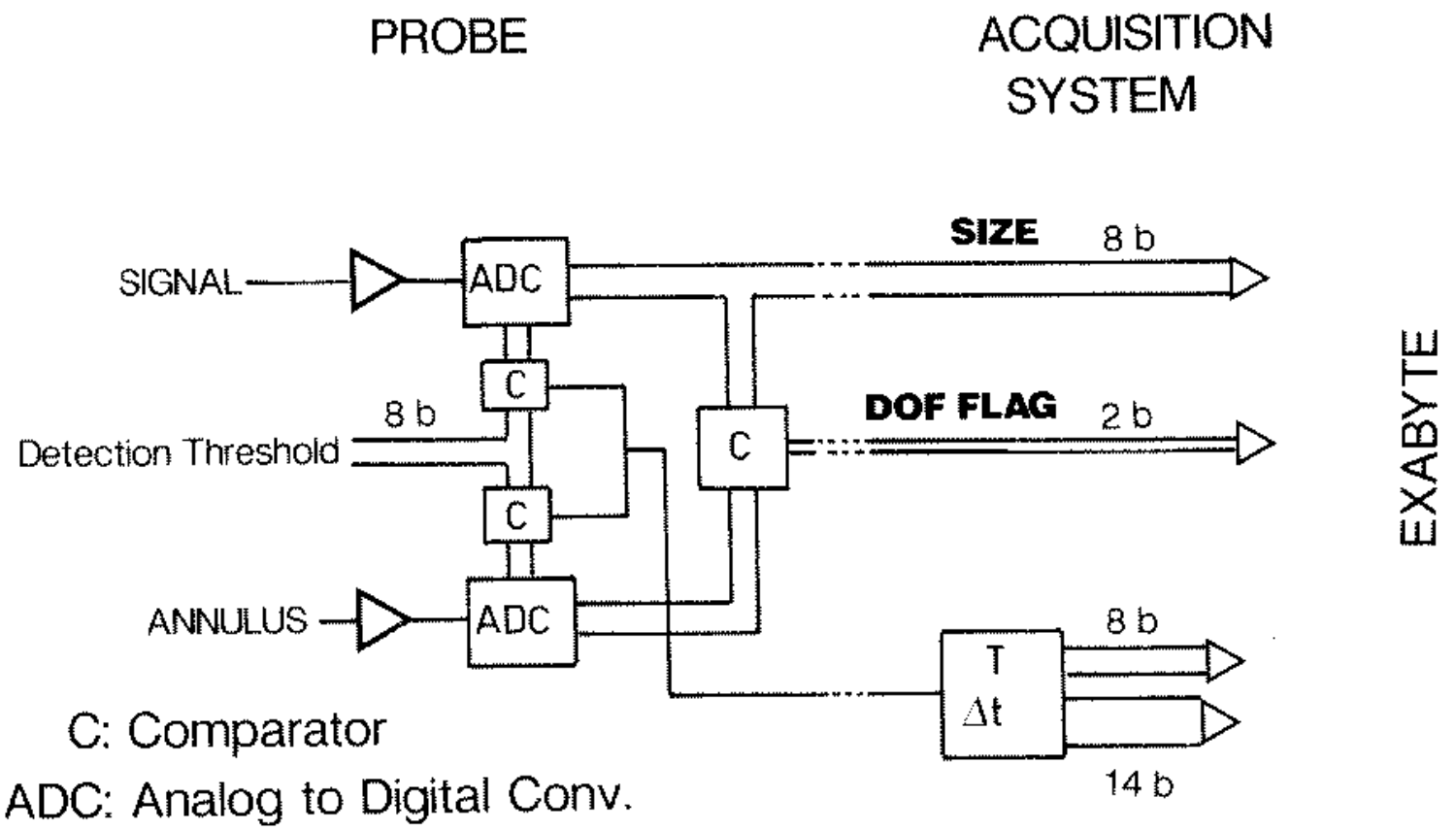

FAST-FSSP versus FSSP-100

Pulse Processing Diagram

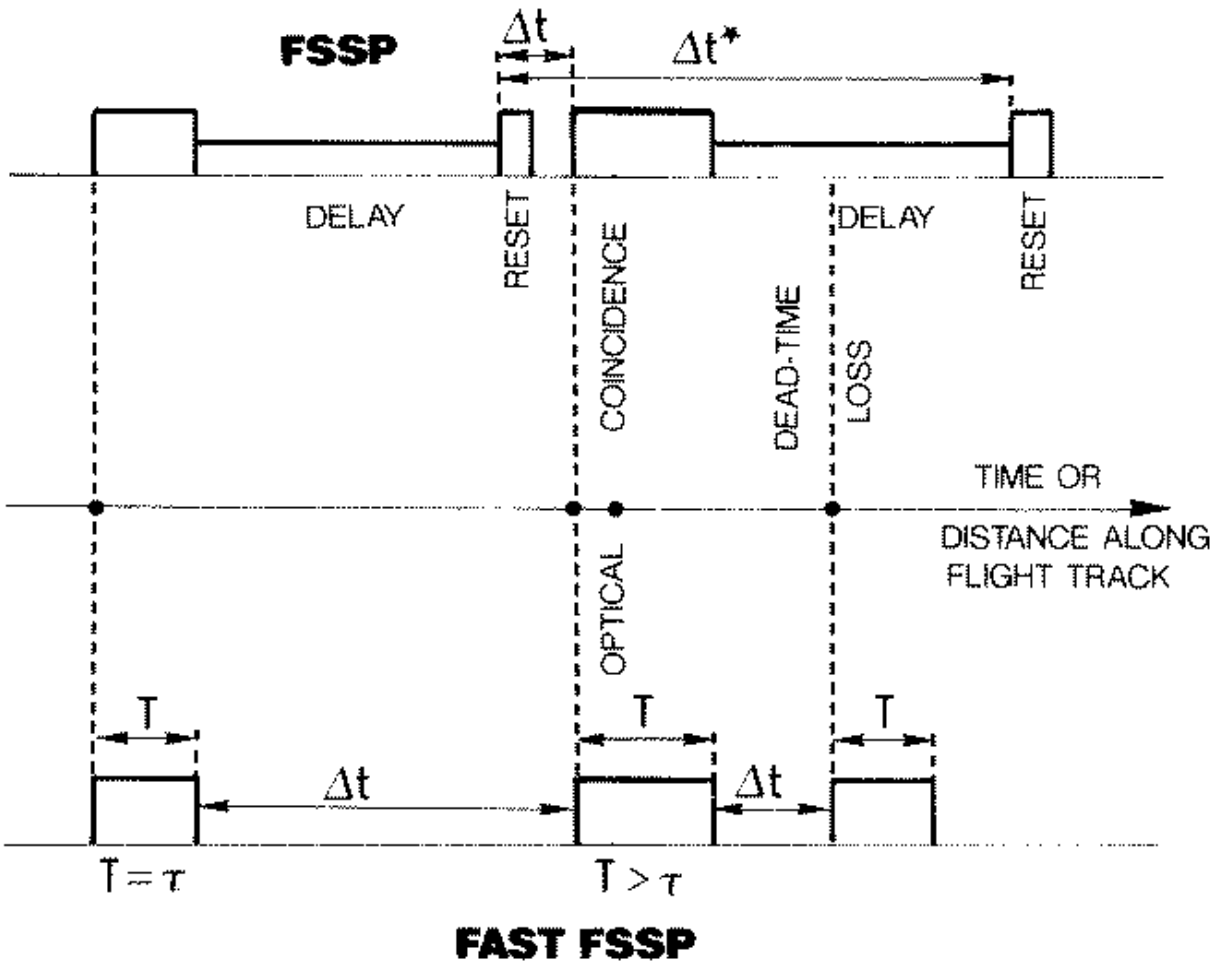

FAST-FSSP *(FSSP-300)*

DOF Selection Optics

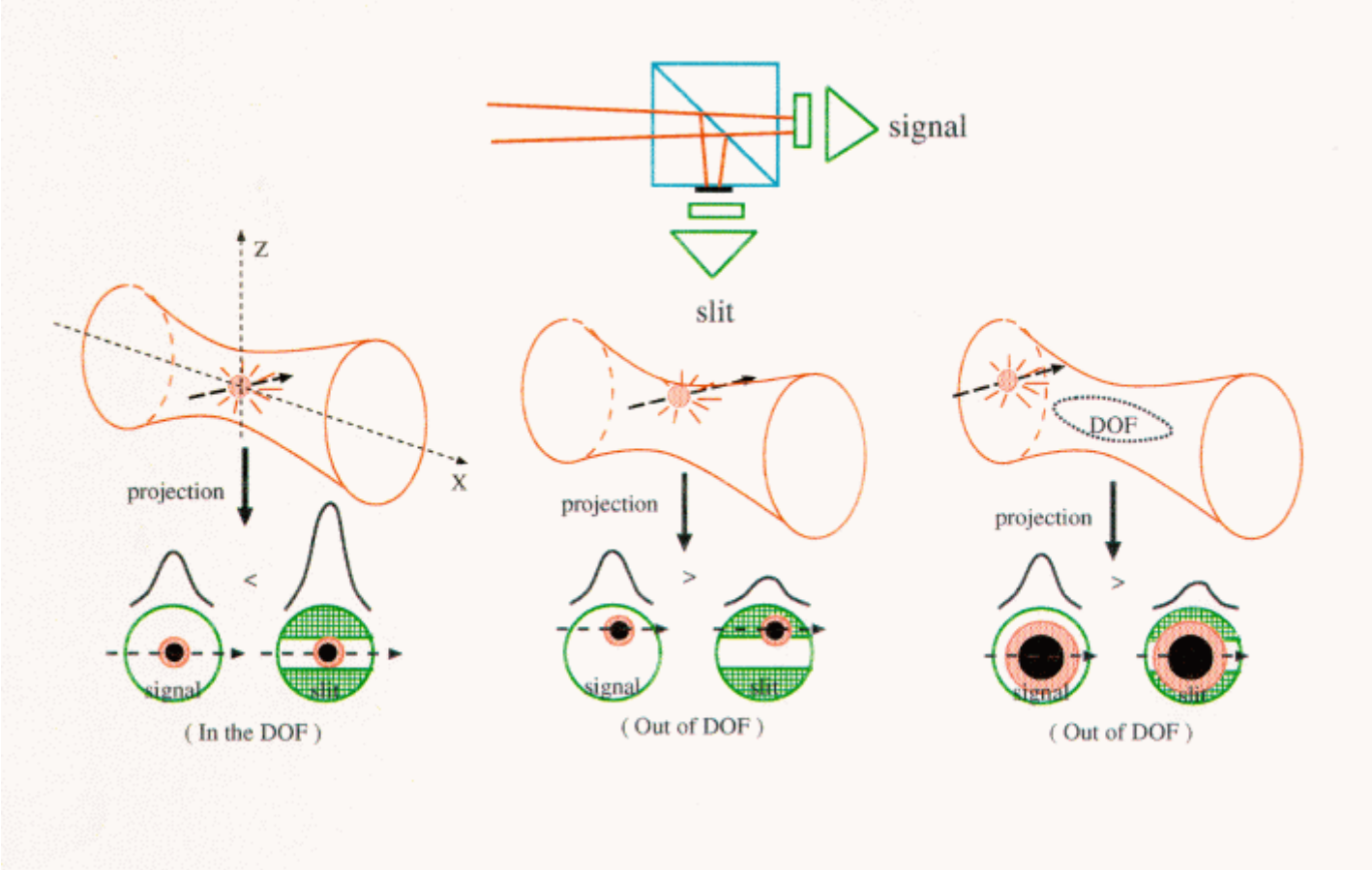

FAST-FSSP

versus FSSP-100

BETTER SIZE RESOLUTION

256 size classes instead of 16

Brenguier, 1993,
J.A.M. 32, 783-793

Pawlowska et al., 1997,
J.A.O.T., 14, 88-104

Brenguier et al. 1998,
J.A.O.T., 15, 1077-1090

Brenguier & Chaumat, 2001,
J.A.S., **58**, 628-641.

Chaumat & Brenguier, 2001,
J.A.S., **58**, 642-654.

Burnet & Brenguier, 2002,
J.A.O.T., **in press**.

➡ Characterization of narrow spectra.

Droplet spectra measurements.

The four probes were mounted on the fuselage of the Meteo-France Merlin-IV during the SCMS inter-calibration flight and they were separated by less than 1.5 m.

The large difference of counting in the first class, between the Meteo-France FSSP-100 and the ones from UWYO and NCAR, is due to the different settings of the velocity rejection module (delay mode on for MF, delay mode off for UWYO and NCAR).

This example shows that the FAST-FSSP is able to measure a narrow spectrum, with about 50 % of the droplet number density within one class of the FSSP-100.

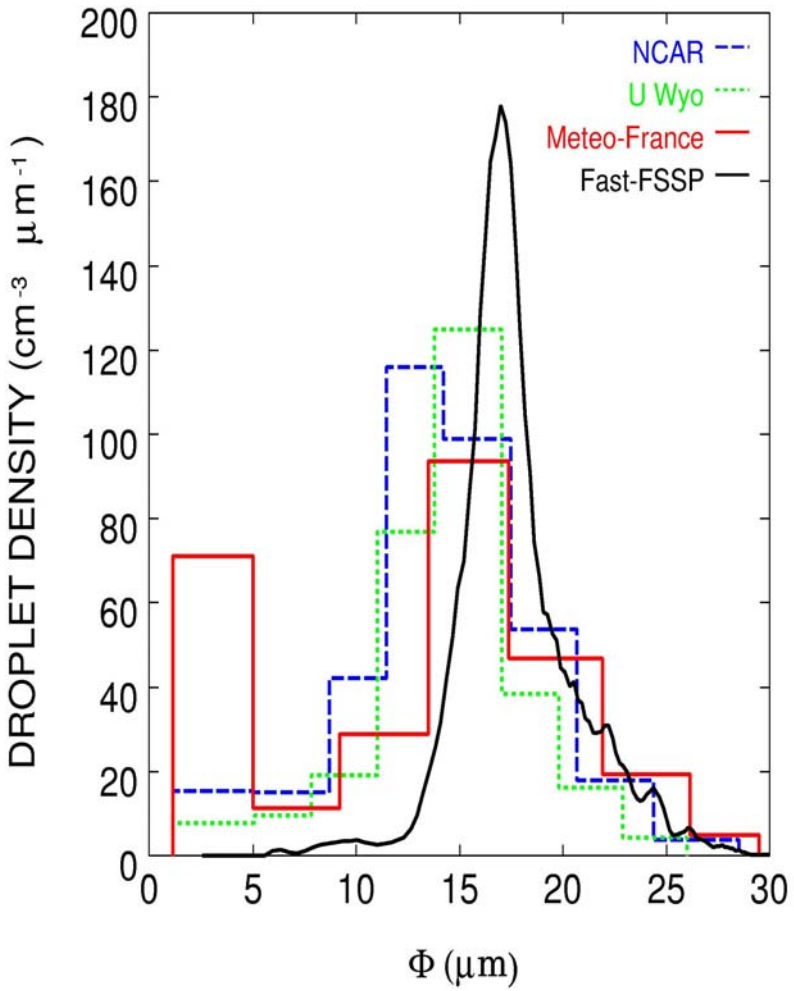

Fig. 1: Comparison of droplet spectra measurements with the FAST-FSSP and three FSSP-100

FAST-FSSP

versus FSSP-100

BETTER SIZE RESOLUTION

256 size classes instead of 16

Brenguier, 1993,
J.A.M. 32, 783-793

Pawlowska et al., 1997,
J.A.O.T., 14, 88-104

Brenguier et al. 1998,
J.A.O.T., 15, 1077-1090

Brenguier & Chaumat, 2001,
J.A.S., **58**, 628-641.

Chaumat & Brenguier, 2001,
J.A.S., **58**, 642-654.

Burnet & Brenguier, 2002,
J.A.O.T., **in press**.

➡Self-calibration technique based on ambiguities of Mie forward scattering.

Self Size calibration

The frequency distribution of pulse amplitude, averaged over a whole flight duration, after removal of the main spectrum component shows values of amplitude that are more frequently counted.

They correspond to the ambiguous sections of the Mie response curve, that are located at fixed values of droplet diameter

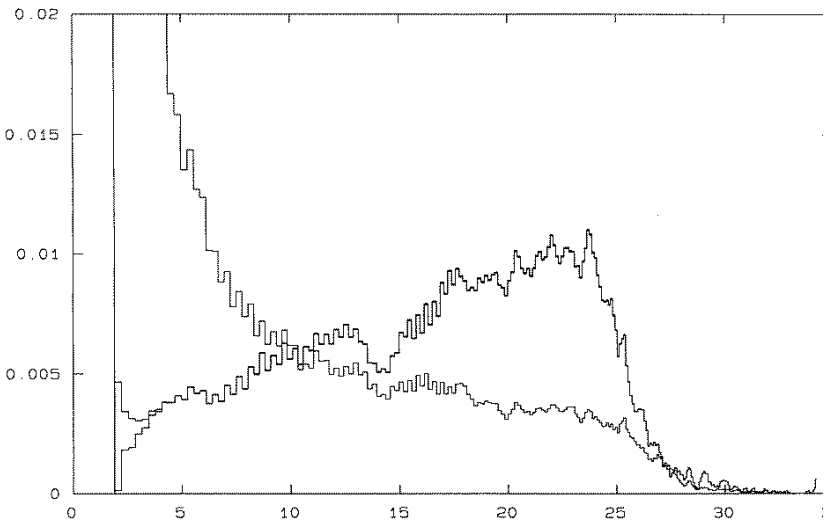

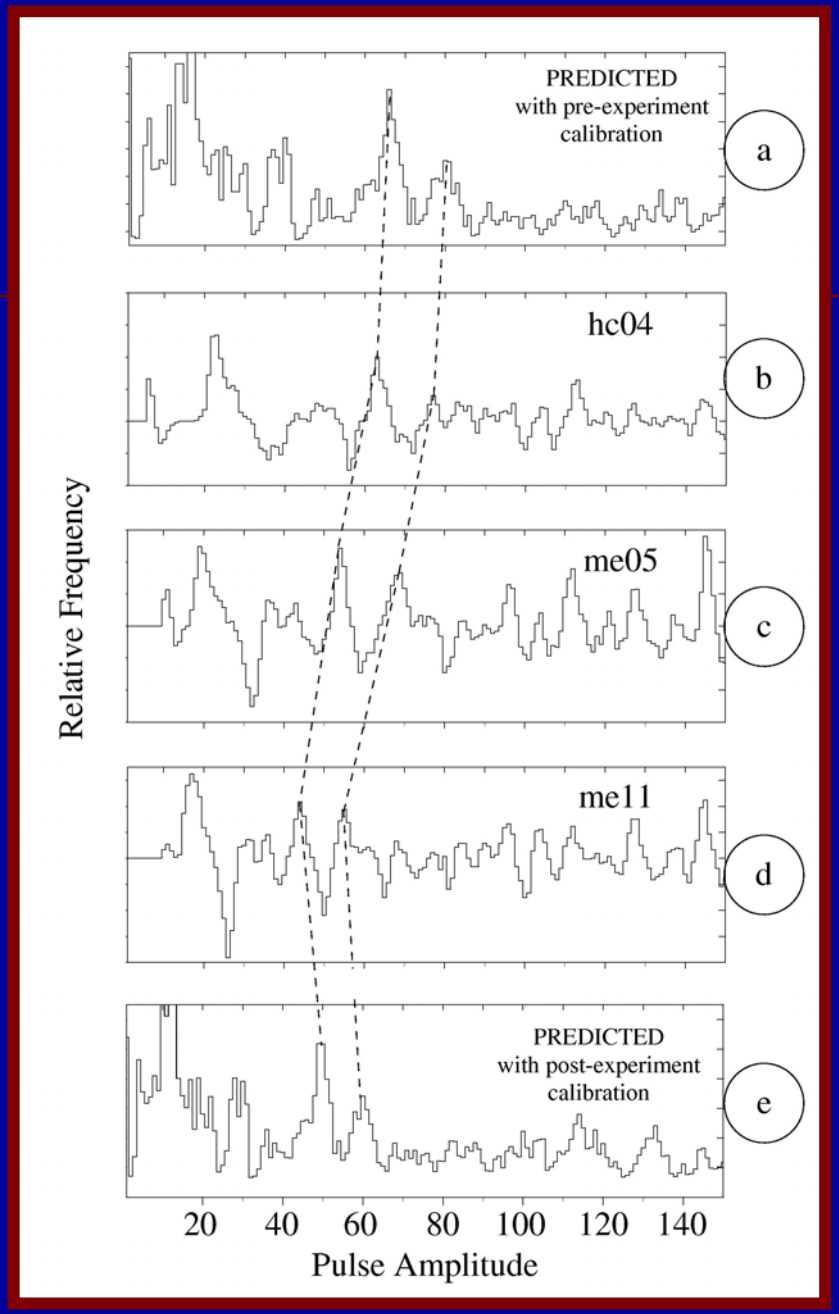

Self Size calibration

The most frequently measured values of pulse amplitude for each flight are plotted against values corresponding to a standard calibration.

The linear fit provides the corrections in gain and offset of the size calibration (amplitude to droplet diameter relationship)

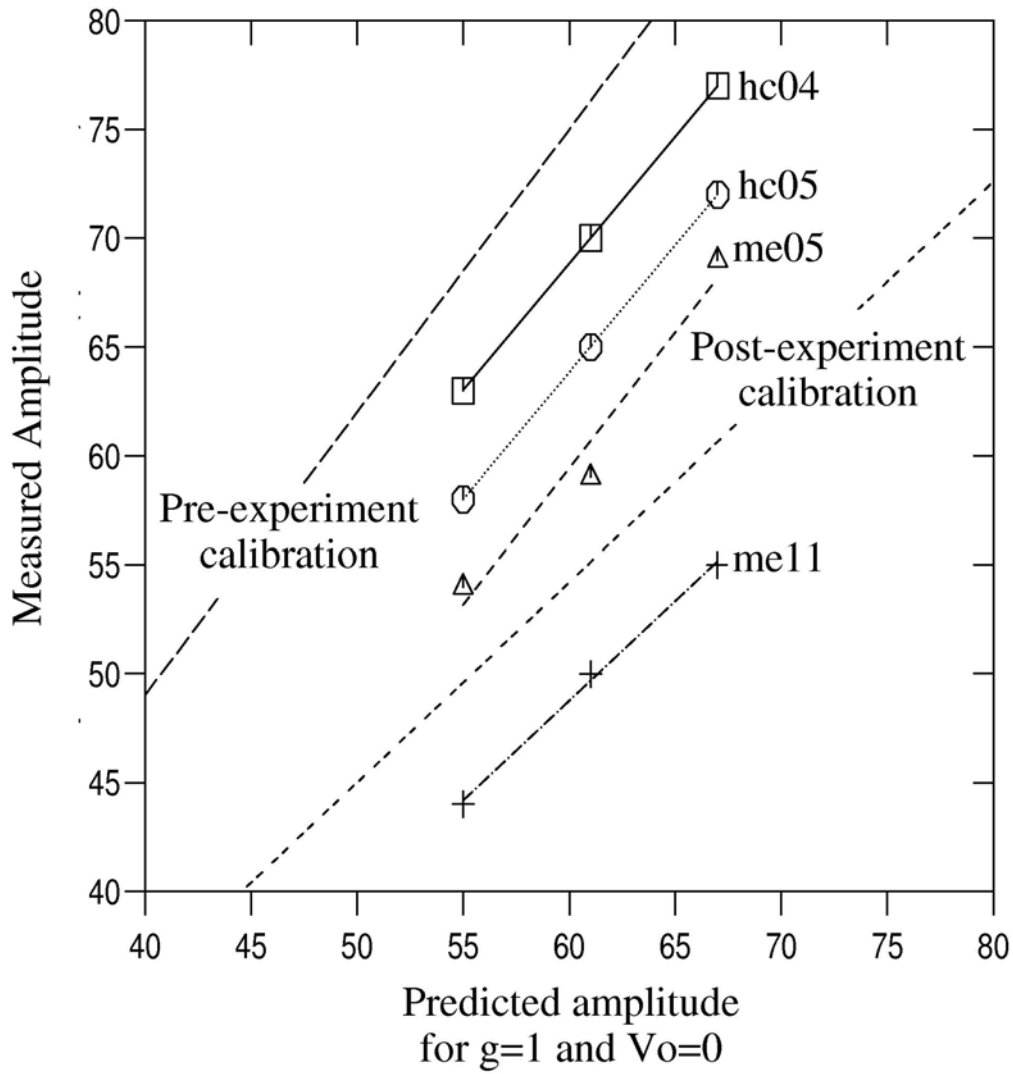

FAST-FSSP

versus FSSP-100

Recording of Pulse Amplitude (A)
And Pulse Duration (T) (1/16 µs),
for each detected particle

➡ The conditional frequency distribution of the measured amplitude versus pulse duration provides a more reliable selection of particles in Depth of Field.

➡ The frequency distribution of the measured pulse duration provides accurate estimation of droplet concentration, corrected for coincidence losses. No dead-time losses.

Brenguier, 1993,
J.A.M. 32, 783-793

Pawlowska et al., 1997,
J.A.O.T., 14, 88-104

Brenguier et al. 1998,
J.A.O.T., 15, 1077-1090

Brenguier & Chaumat, 2001,
J.A.S., **58**, 628-641.

Chaumat & Brenguier, 2001,
J.A.S., **58**, 642-654.

Burnet & Brenguier, 2002,
J.A.O.T., **in press**.

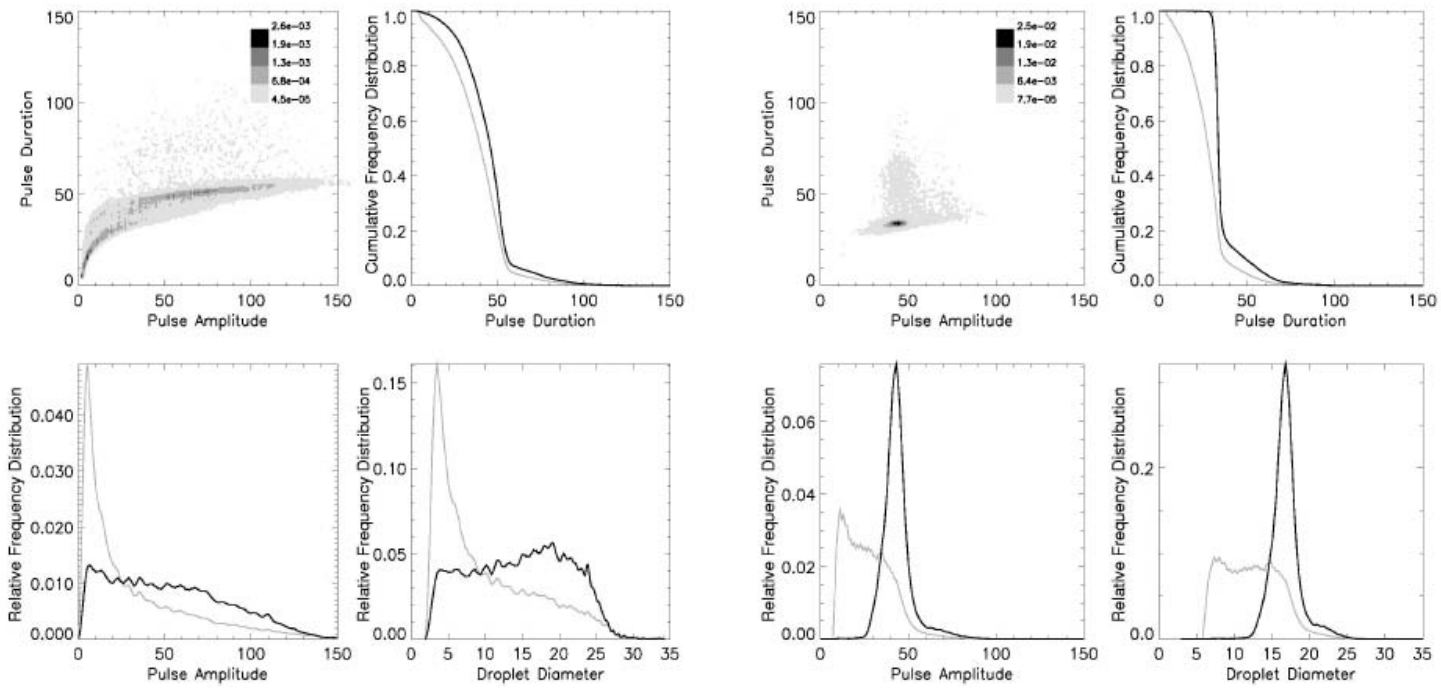

Frequency distributions of pulse duration T and amplitude A.
Thin line: all detections; thick line DOF selected pulses

With the standard optics, the conditional T/A freq. dist. shows a large proportion of detections with low A and short T. They correspond to droplets crossing the laser beam edge. This is confirmed by the T freq. dist. in DOF that is typical of particles crossing a cylindrical beam. The velocity rejection module aims at rejecting those edge effects. However it is based on rejection of all the detections with T longer than the mean. Because of the slight T/A slope, this procedure preferentially rejects small particles. The delay mode aims at compensating this trend, but it overestimates the proportion of small particles in the first class (previous figure).

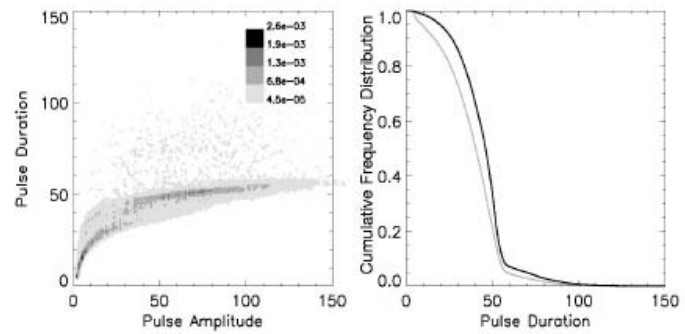

FSSP-100 Optics
(Annulus)

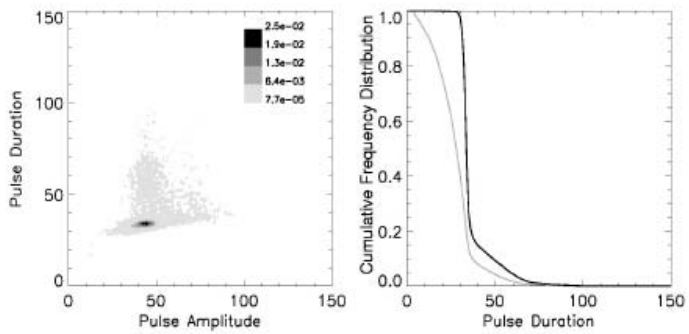

FSSP-300 Optics
(Slit)

Frequency distributions of pulse duration T and amplitude A.
Thin line: all detections; thick line DOF selected pulses

The SLIT provides optical selection along the depth of field and across the laser beam. The statistics on the right hand side demonstrates that edge effects are correctly rejected. The distribution of pulse duration in DOF is typical of particles crossing the central portion of the beam. The resulting amplitude (diameter) spectra are narrower with the SLIT optics.

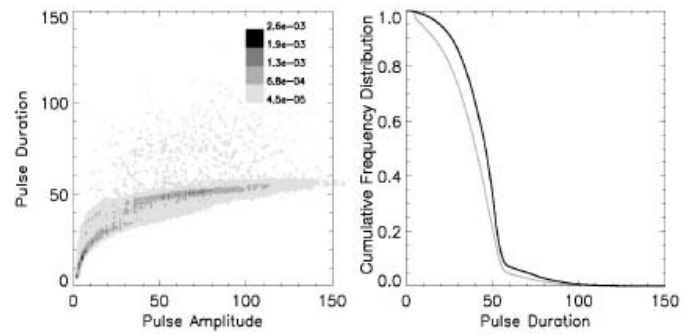

FSSP-100 Optics
(Annulus)

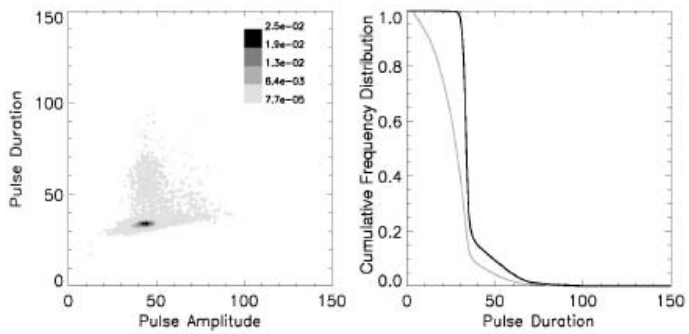

FSSP-300 Optics
(Slit)

Frequency distributions of pulse duration T and amplitude A.
Thin line: all detections; thick line DOF selected pulses

Coincidence effects are noticeable in both distributions of pulse duration with the tail towards long duration values, that can easily be rejected. The coincidences of particles entering the beam simultaneously are not characterized by a long pulse duration but rather a large pulse amplitude, and they produce an overestimation of large particles. They cannot be detected by either the standard or the new optics, and they must be statistically corrected.

FAST-FSSP

versus FSSP-100

Recording of arrival time (1/16 µs)
for each detected particle

Brenguier, 1993,
J.A.M. 32, 783-793

Pawlowska et al., 1997,
J.A.O.T., 14, 88-104

Brenguier et al. 1998,
J.A.O.T., 15, 1077-1090

Brenguier & Chaumat, 2001,
J.A.S., **58**, 628-641.

Chaumat & Brenguier, 2001,
J.A.S., **58**, 642-654.

Burnet & Brenguier, 2002,
J.A.O.T., **in press**.

➡ The frequency distribution of the measured inter-arrival time provides a redundant estimation of droplet concentration, corrected for coincidence losses.

➡Both estimations based on pulse duration and inter-arrival time agree within 5 %.

FAST-FSSP

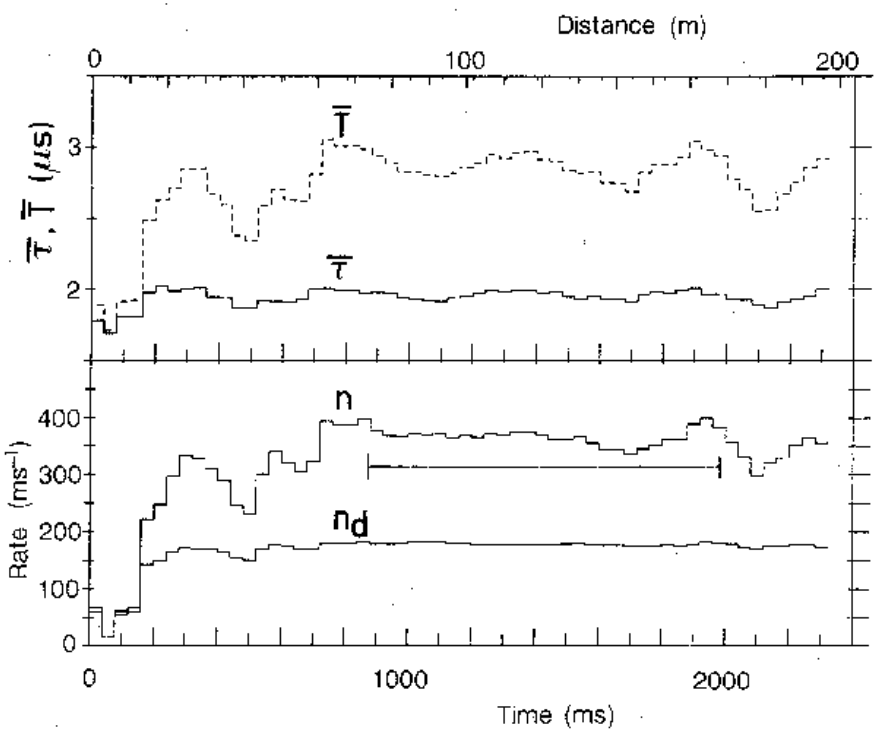

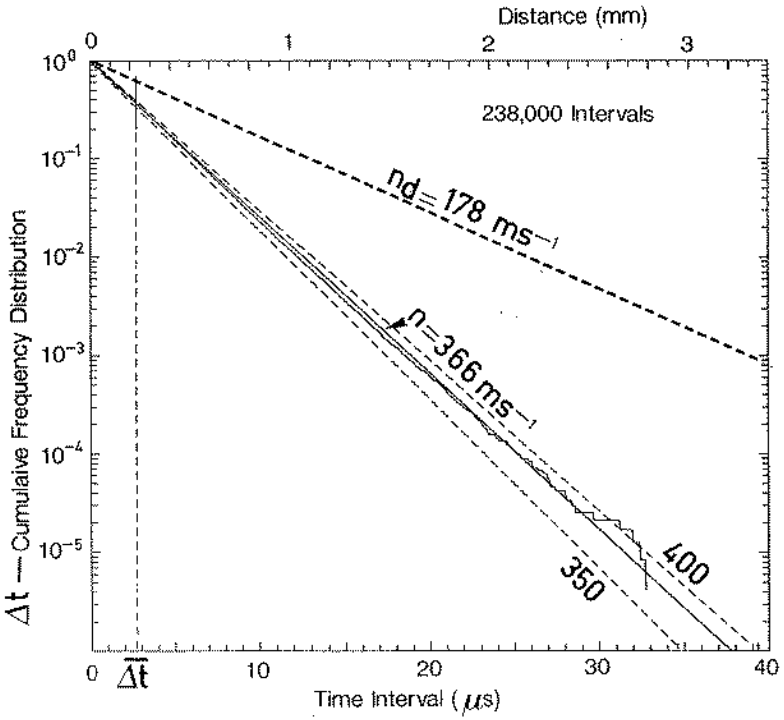

$$n = \frac{n_d}{1 - n_d \overline{T}}$$

$$\tau = \frac{1}{n} \ln\left(\frac{n}{n_d}\right)$$

$$P(\Delta t > \Delta t') = e^{-n\Delta t'}$$

FAST-FSSP

versus FSSP-100

Recording of arrival time (1/16 µs)
for each detected particle

Brenguier, 1993,
J.A.M. 32, 783-793

Pawlowska et al., 1997,
J.A.O.T., 14, 88-104

Brenguier et al. 1998,
J.A.O.T., 15, 1077-1090

Brenguier & Chaumat, 2001,
J.A.S., **58**, 628-641.

Chaumat & Brenguier, 2001,
J.A.S., **58**, 642-654.

Burnet & Brenguier, 2002,
J.A.O.T., **in press**.

➡ The series of arrival times allow Bayesian estimation of droplet concentration at small scale and the detection of cm scale transitions in the droplet spatial distribution.

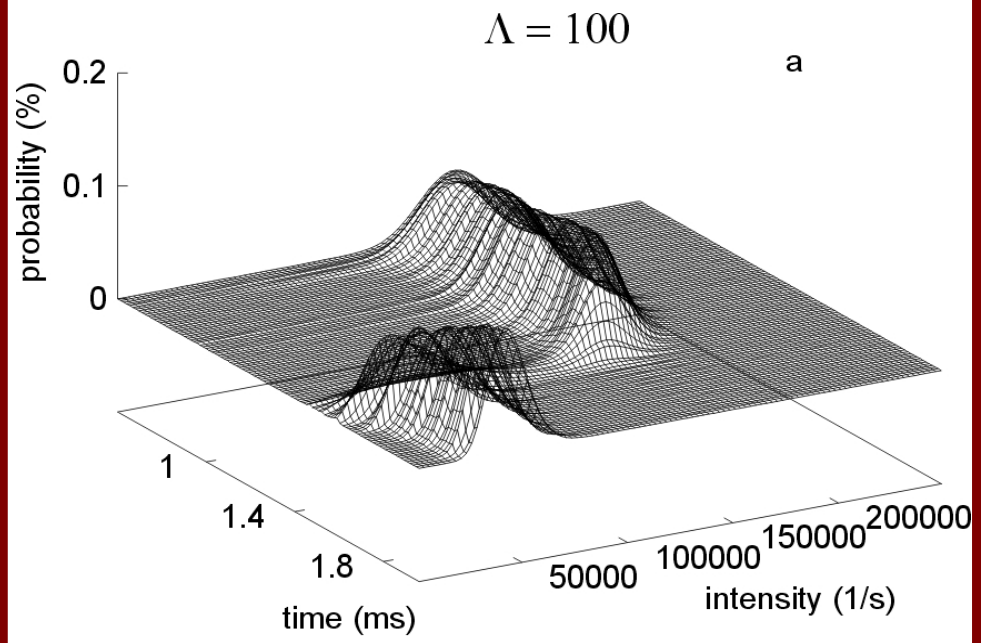

Bayesian Estimation

The probability density function of the particle rate is updated at each particle arrival time with a stochastic differential optimal estimation

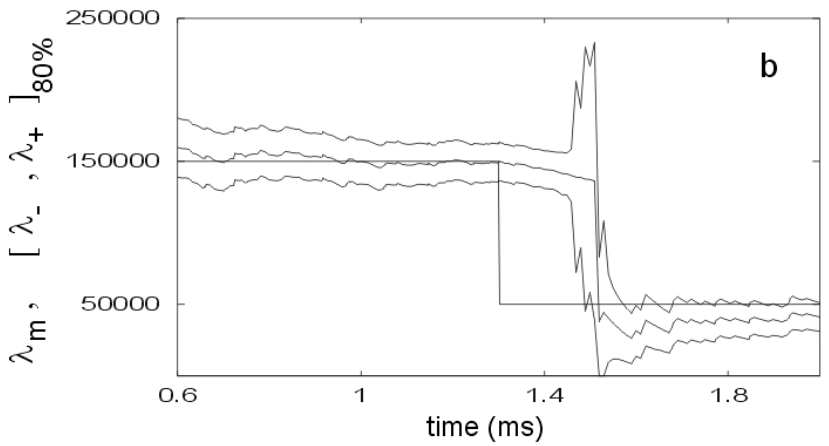

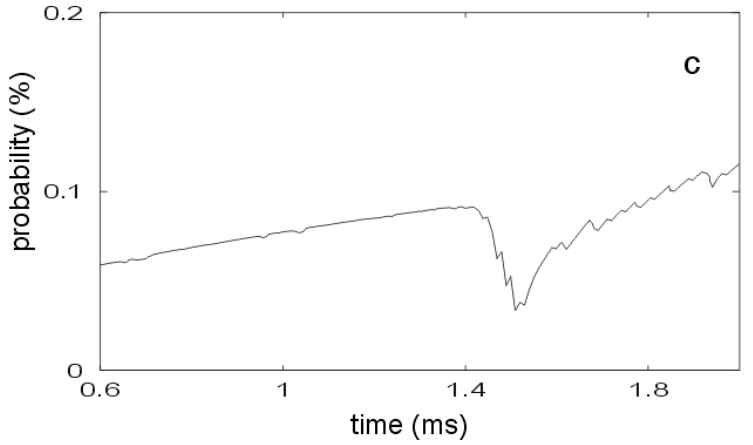

Bayesian Filter

In this simulation, particles are arriving randomly with a mean rate of 150000 s^{-1}, sudenly falling down to 50000 s^{-1}.

On the right, the solid lines show the most probable rate, with the 80% confidence interval.

0.2 ms, that is about 10 particles, is enough for the estimation to detect the jump.

Bayesian Centered Filter

In this simulation, particles are arriving randomly with a mean rate of 50000 s^{-1}, suddenly jumping up to 100000 s^{-1}, for a duration of 1 and 0.65 ms respectively.

The solid lines show the most probable rate, with the 80% confidence interval.

A jump duration of 1 ms, i.e. about 100 particles, is enough for the optimal estimation to detect the jump.

At a duration of 0.65 ms, the most probable rate is not changed, but the 80% confidence interval reveals that particle statistics have changed during that interval.

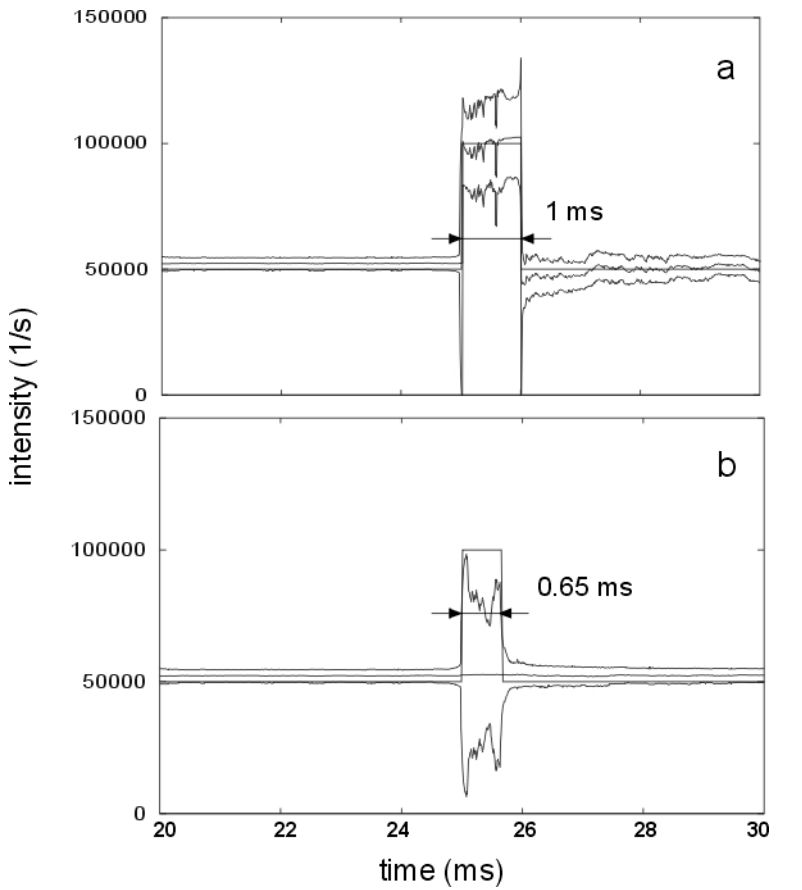

PVM-100 – Fast-FSSP comparison at the small scale

LWC measurements made with the PVM-100 at 1000 Hz (10 cm spatial resolution) and the FAST-FSSP.

Top graph shows the comparison with FAST-FSSP LWC calculated at 100 Hz. At a higher sampling frequency, the number of droplets per sample is too small for a significant estimation of LWC and noise due to randomness of counting becomes larger than physical fluctuations of LWC.

Bottom graph shows the FAST-FSSP LWC calculated at 1000 Hz with the non-linear optimal estimator of Pawlowska et al. (1997), for two selected sections of sharp transitions in LWC.

Both the PVM and FAST-FSSP data exhibit remarkable simultaneity in the detection of the sharp transitions and cm scale LWC fluctuations.

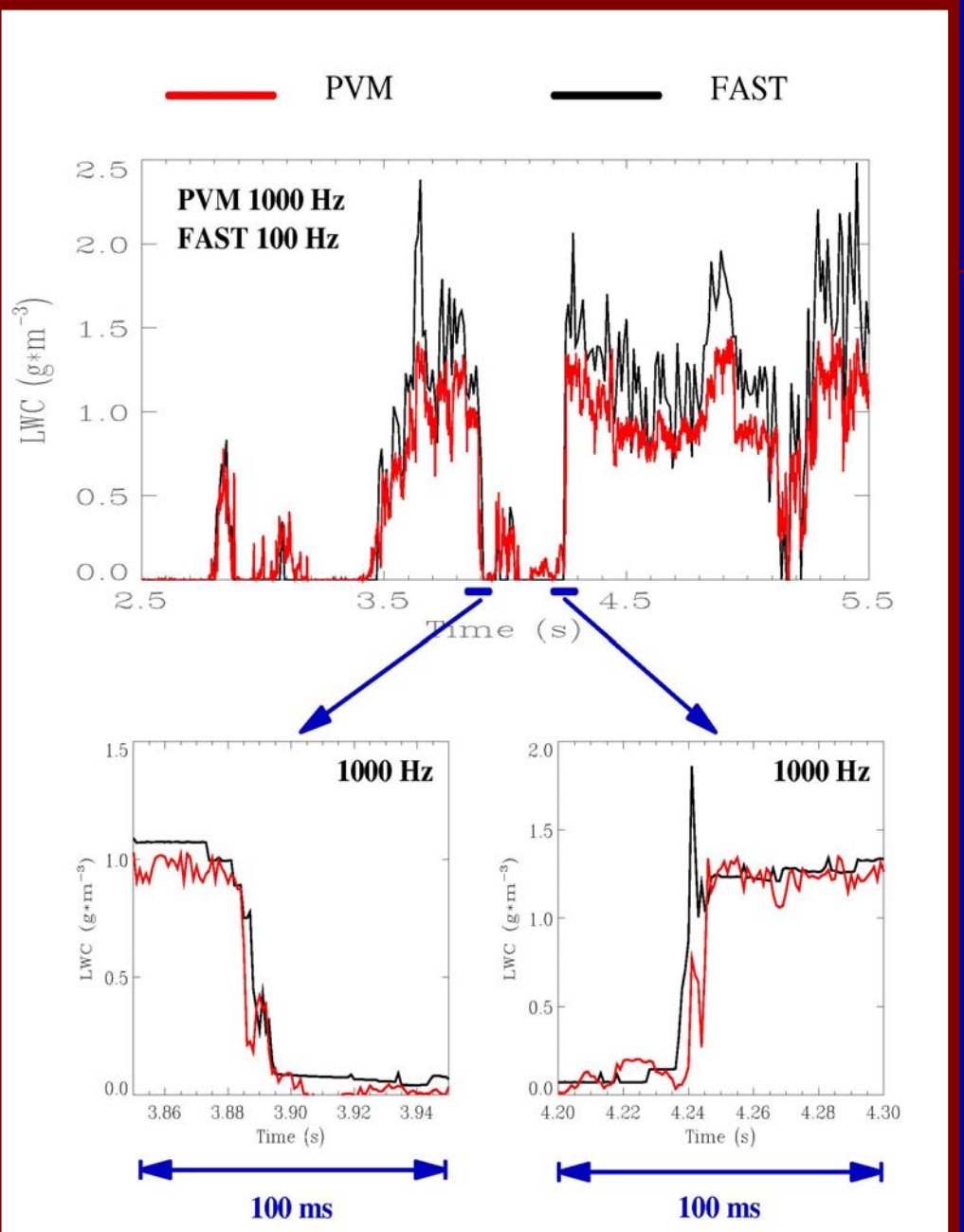

FAST-FSSP

versus FSSP-100

Recording of arrival time (1/16 µs)
for each detected particle

Brenguier, 1993,
J.A.M. 32, 783-793

Pawlowska et al., 1997,
J.A.O.T., 14, 88-104

Brenguier et al. 1998,
J.A.O.T., 15, 1077-1090

Brenguier & Chaumat, 2001,
J.A.S., **58**, 628-641.

Chaumat & Brenguier, 2001,
J.A.S., **58**, 642-654.

Burnet & Brenguier, 2002,
J.A.O.T., **in press**.

➡The series of arrival times allow calculation of statistical properties of the droplet spatial distribution: Poisson and Fishing test.

Droplet spatial distribution.

The series of inter-arrival time is used to analyse the droplet spatial distribution.

Top: The series of counts are cumulated over sections of various length scales, from 2 mm to 100 mm corresponding to mean number of counts from 2 to 100. The statistics of counting is compared to the Poisson statistics. This cloud traverse, selected in an adiabatic core shows no deviation from the Poisson statistics. It is particularly homogeneous down to the mm scale.

Bottom: Four similar cloud traverses are analysed with the variance test at various length scales, from 2 mm to 20 m. Most of the cm scale values are within ± 3 that characterize the 97 confidence interval for a homogeneous Poisson process. This feature confirms that the selected adiabatic cores are homogeneous at the cm scale.

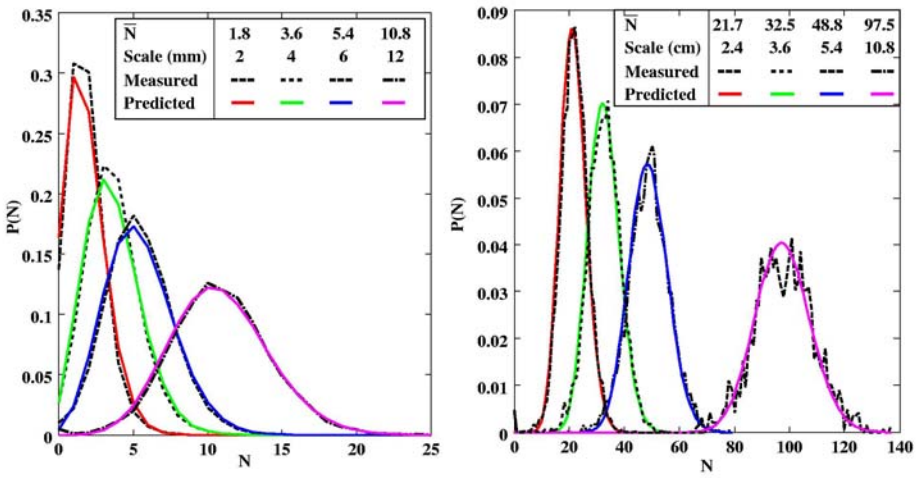

Counting statistics at different length scales compared to the Poisson statistics for one cloud traverse

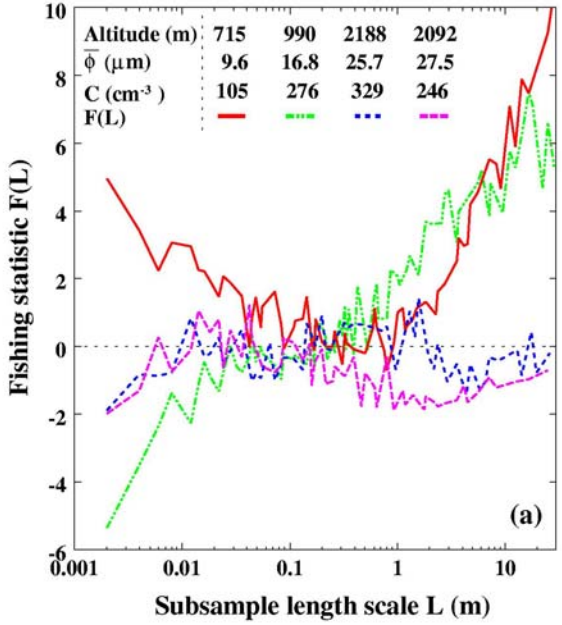

Fishing test for 4 cloud traverses

FAST-FSSP

versus FSSP-100

AN EXAMPLE OF FAST-FSSP DATA ANALYSIS

Brenguier, 1993,
J.A.M. 32, 783-793

Pawlowska et al., 1997,
J.A.O.T., 14, 88-104

Brenguier et al. 1998,
J.A.O.T., 15, 1077-1090

Brenguier & Chaumat, 2001,
J.A.S., **58**, 628-641.

Chaumat & Brenguier, 2001,
J.A.S., **58**, 642-654.

Burnet & Brenguier, 2002,
J.A.O.T., **in press**.

Time evolution of a convective cell.

At 2170 m, the temperature in the cell is warmer than in the environment and the vertical velocity is upward, except on the sides, where the air is at rest and the temperature slightly colder than the environment. The cloud core is homogeneous (FT(0.01) and FT(1) smaller than 3, the concentration is maximum and the spectrum narrow. On the sides, FT values increase progressively to 1000, droplet concentration is diluted and spectra are broader. This features are typical of an ascending vortex, with mixing occurring on both sides of the cell.

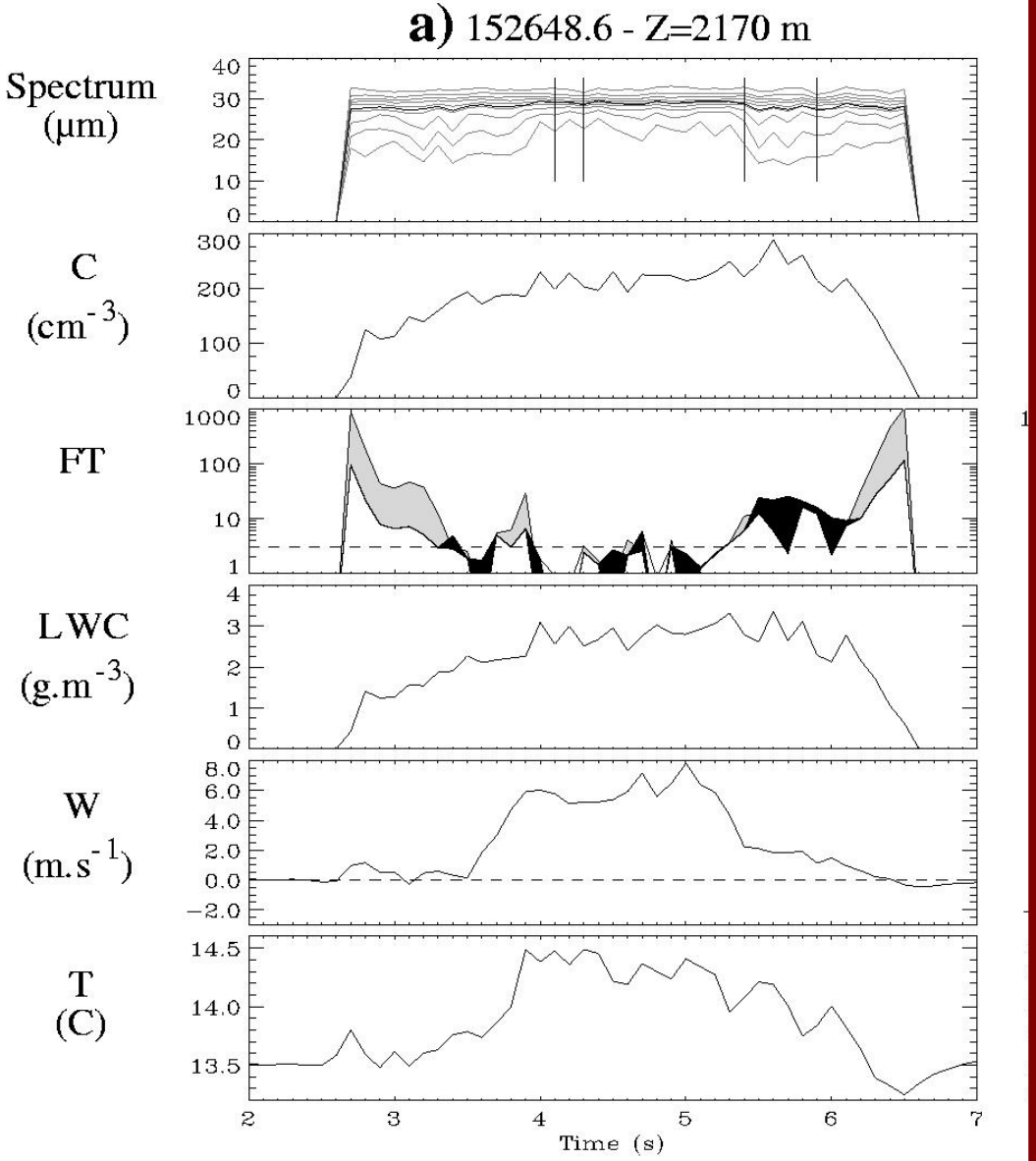

Time evolution of a convective cell.

As the cell penetrates the inversion layer, the temperature becomes colder than the environment, starting from the sides; the velocity decreases and becomes slightly negative; the number concentration is progressively diluted; the spectra become broader and the heterogeneities are penetrating inside the cell, with FT values larger than 3, though lower than at the beginning of the ascent (100 max instead of 1000).

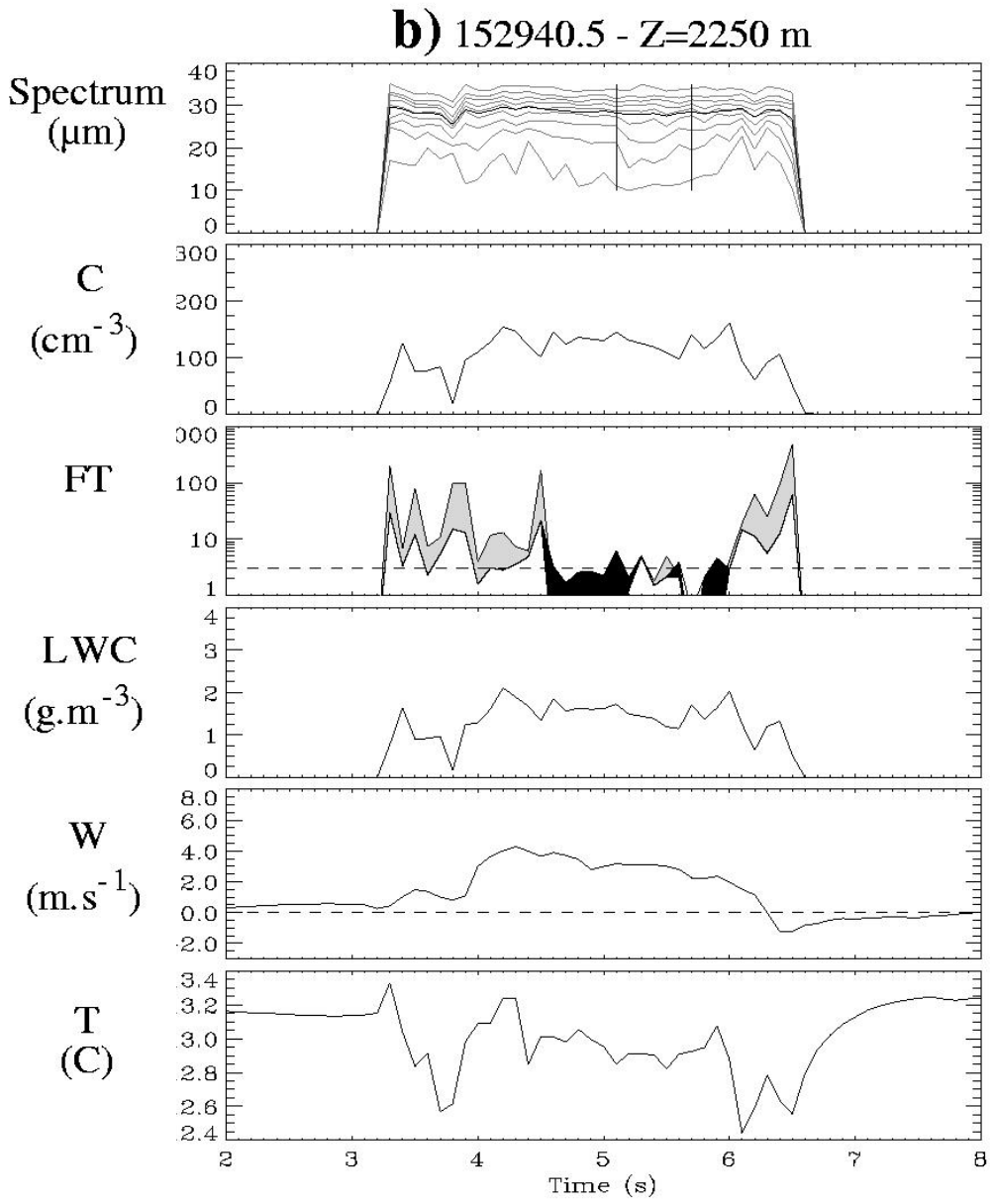

Time evolution of a convective cell.

As the cell penetrates the inversion layer, the temperature becomes colder than the environment, starting from the sides; the velocity decreases and becomes slightly negative; the number concentration is progressively diluted; the spectra become broader and the heterogeneities are penetrating inside the cell, with FT values larger than 3, though lower than at the beginning of the ascent (100 max instead of 1000).

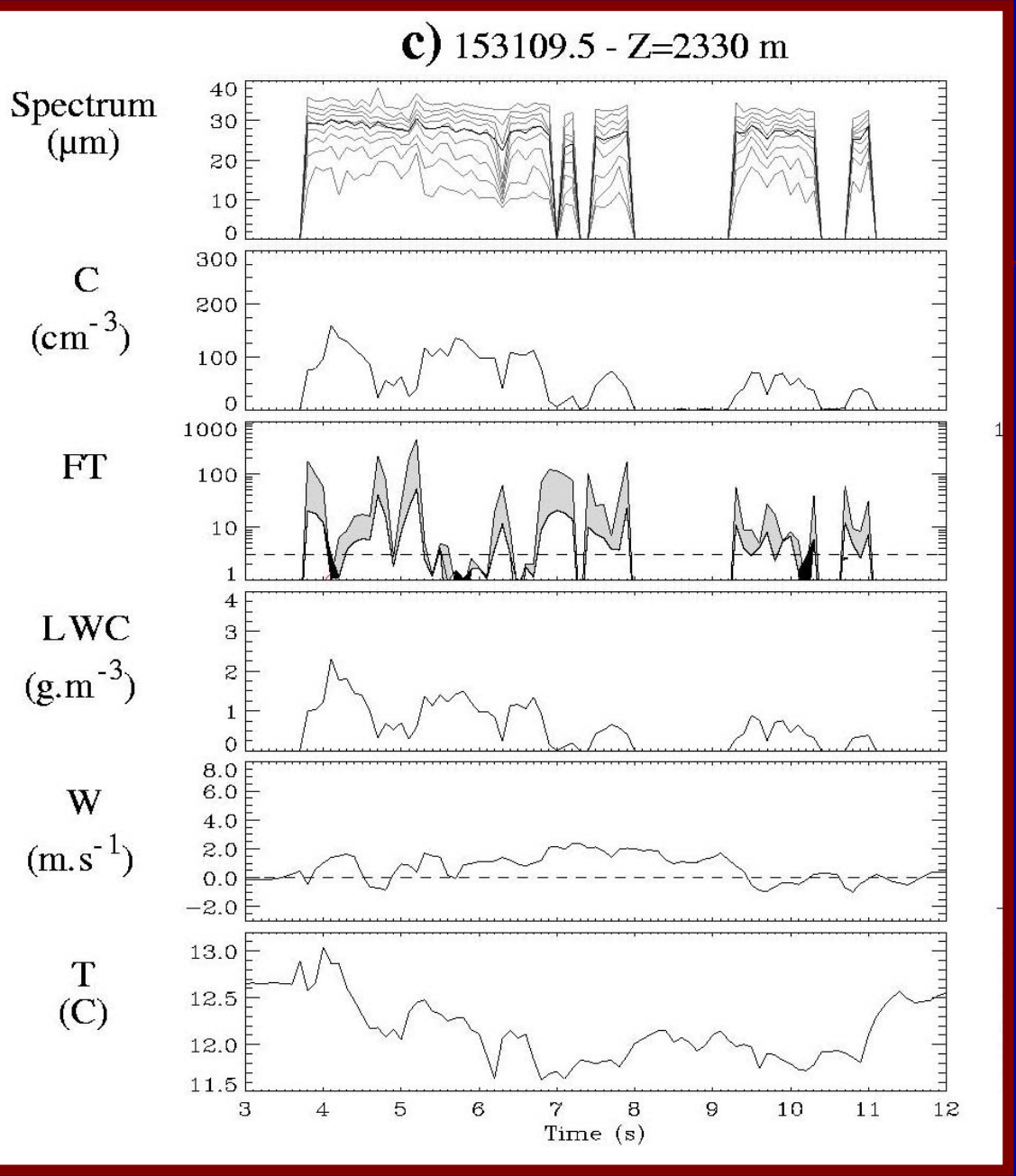

Time evolution of a convective cell.

As the cell penetrates the inversion layer, the temperature becomes colder than the environment, starting from the sides; the velocity decreases and becomes slightly negative; the number concentration is progressively diluted; the spectra become broader and the heterogeneities are penetrating inside the cell, with FT values larger than 3, though lower than at the beginning of the ascent (100 max instead of 1000).